Eur Biophys J (1998) 27: 341–351 

ARTICLE

**Z. Mamdouh · M.-C. Giocondi · C. Le Grimellec**

# In situ determination of intracellular membrane physical state heterogeneity in renal epithelial cells using fluorescence ratio microscopy

Received: 3 June 1997 / Revised version: 6 March 1998 / Accepted: 7 March 1998

**Abstract** 6-Lauroyl-2-dimethylaminonaphtalene (laurdan) shows a spectral sensitivity to the lipid phase state with a 50 nm red shift of the emission maximum when passing from the gel to the liquid crystalline phase. This spectral sensitivity allows one to determine the membrane physical state using Generalized Polarization (GP). In the present experiments, we used fluorescence ratio imaging microscopy to determine the laurdan GP in living kidney cells. Two renal epithelial cells lines, MDCK and LLC-PK1 cells, and CV-1 cells, a fibroblast-like renal cell line were investigated. In these cells, laurdan labels both the plasma membrane and intracellular membranes. Comparison of spectrofluorimetry and fluorescence ratio imaging data obtained from liposomes and cells suspensions labeled with laurdan demonstrates that the GP can be accurately determined using common fluorescence microscopy equipment. The GP mean values determined from individual cells varied from 0.2 to 0.4 for the epithelial cells as compared to 0.0–0.1 for CV1 cells. Using living MDCK cells grown as a monolayer, the GP maps indicated that, within a single cell, the intracellular GP values varied from 0.0 to 0.6, i. e., from the equivalent of a liquid-crystalline state to a gel or a lipid-ordered state, and that there was a marked heterogeneity in the spatial distribution of the GP values. To further characterize this intracellular heterogeneity, co-localization experiments with specific organelle markers were undertaken. The results strongly suggest that in intact cells at physiological temperature, GP values decrease in the following order: plasma membranes > endosomes > mitochondria > Golgi apparatus.

Z. Mamdouh
Institut National de la Santé et de la Recherche Médicale,
U. 426, Faculté Xavier Bichat, Paris, France

M.-C. Giocondi · C. Le Grimellec (✉)
Centre de Biochimie Structurale,
Institut National de la Santé et de la Recherche Médicale,
U. 414, I. U. R. C., 75 Rue de la Cardonille,
F-34093 Montpellier Cedex 05, France

**Key words** Living MDCK cells · Laurdan · Generalized polarization · Endosomes · Golgi · Mitochondria

**Abbreviations** *FRIM* Fluorescence ratio imaging microscopy · *$C_6$-NBD-Cer* N-[7-(4-nitrobenzo-2-oxa-1,3-diazole)]-6-aminohexanoyl-D-erythro-sphingosine · *Laurdan* 6-dodecanoyl-2-dimethylaminonaphtalene · *TMA-DPH* 1-4[-(trimethylamino)phenyl]-6-phenylhexa-1,3,5-triene · *DMPC* Dimyristoylphosphatidylcholine

## Introduction

Although the mechanism(s) involved are still not clearly established, membrane lipids modulate the activity of numerous membrane proteins (for reviews see Shinitzky 1984; Gordon and Mobley 1985; Le Grimellec et al. 1992; Mouritsen and Bloom 1993; Yeagle 1993). Most of the studies have focused on lipid-protein interactions in the plasma membrane of cells and both the composition and the physical state of membrane lipids were shown to be involved in the control of protein activities. Similar conclusions were reached from the few studies devoted to lipid-protein interactions in isolated intracellular membranes. The use of probes such as 1-4[-(trimethylamino)phenyl]-6-phenylhexa-1,3,5-triene (TMA-DPH; Prendergast et al. 1981) that remain localized in the plasma membrane of numerous cell types (Khury et al. 1985; Le Grimellec et al. 1988; Storch et al. 1989) allowed the investigation, in situ, of the membrane physical state of living cells and its variation in physiological and pathological conditions (Sheridan et al. 1988; Fiorini et al. 1990; Giocondi et al. 1990; Illinger et al. 1990). Except for recent work where TMA-DPH internalization was used to follow the physical state of endosomes in cells (Illinger and Khury 1994), equivalent studies on intracellular membranes are still lacking. Such in situ studies would present multiple interests: a) purification steps with the possibility of cross-contamination between the different types of intracellular membranes and of alterations in membrane physical state

are avoided; b) variations in the physical state of a defined organelle upon a physiological event, for instance a hormonal stimulation, can be followed; c) membrane changes during intracellular trafficking can be estimated. This last point is of particular interest because it has been proposed that lipid phase separations are involved in the sorting of membrane proteins in epithelial cells (Simons and van Meer 1988).

Laurdan (6-Lauroyl-2-dimethylamino-naphtalene) is a fluorescent probe that has a much higher quantum yield in membranes that in aqueous solutions and which shows a spectral sensitivity to the lipid phase state with a 50 nm red shift of the emission maximum when passing from the gel to the liquid crystalline phase (Parasassi et al. 1990, 1991). This property allows one to determine the physical state of membranes using Generalized Polarization, GP (Parasassi et al. 1990). Laurdan was used to estimate the physical state of isolated renal brush border membranes (Levi et al. 1993) and of the membrane(s) of various living cells in suspension (Parasassi et al. 1992, 1993). In fact, the spectroscopic properties of laurdan report on the local water content in membranes (Parasassi and Gratton 1995) which is markedly dependent on their physical state. Recently, Yu et al. (1996) have determined the laurdan GP in intact mouse fibroblasts. They reported that laurdan labels not only the plasma membrane, but also the intracellular membranes. They observed high GP values for the plasma membrane and low GP values at the level of the nuclear membrane. The equipment used for their experiments was a two-photon scanning microscope, based on a Ti-sapphire laser pumped by an Ar laser. Such equipment is rather expensive and few laboratories can afford it. On the other hand, numerous laboratories are equipped for fluorescence ratio imaging microscopy (FRIM), a technique which has many applications in cell biology (Bright et al. 1989; Dunn et al. 1994). We therefore used FRIM on renal cells in culture labeled with laurdan to determine the physical state of their intracellular membranes. Co-localization experiments with $DIOC_{(6)}$, a marker of mitochondria (Terasaki 1989; Bergeron et al. 1994), NBD-ceramide or BODIPY TR ceramide, two markers of the Golgi apparatus (Lipsky and Pagano 1985; Pagano et al. 1991), and rhodamine labeled bovine serum albumin as a marker for endosomes, were used to establish the identity of the intracellular membranes probed.

## Materials and methods

### Materials

Plasticware was purchased from Costar (Dutscher, France). Glass coverslips were obtained from Polylabo (France). Culture media were from Gibco BRL (France). Hormones, growth factors, and BSA-Rhodamine were from Sigma. The other fluorescent probes were purchased from Molecular Probes (Eugene, OR). All other reagents were of analytical grade.

### Cell culture

The two renal epithelial cell lines, MDCK and LLC-PK1, were grown to confluence (4–5 days) on 28 mm diameter glass coverslips in Petri dishes, in a mixture of serum-free fully defined medium (SFFD) made of 1 : 1 (v/v) Dulbecco's modified Eagle's medium (DMEM) and Ham's F-12 as previously described (Giocondi et al. 1995). For CV-1 cells, a kidney fibroblastic-like cell line, the growth medium consisted of DMEM supplemented with glucose (50 mM), L-glutamine (2 mM), 100 U/ml penicillin, 100 μg/ml streptomycin and 10% fetal calf serum. All cell lines were grown at 37 °C in a 5% $CO_2$–95% air atmosphere.

### Cell labeling

*Laurdan labeling.* Cells on glass coverslips were incubated for 60 min at 37 °C, in the dark, with 2 μM laurdan added to SFFD from a 2 mM stock solution in dimethyl formamide. The laurdan stock solution was renewed every 3–4 weeks. Cells were then washed 4 times with phosphate saline buffer (PBS, pH 7.4) pre-equilibrated at 37 °C and placed in a thermostatted chamber (Medical Systems, Corp., Greenvale, NY) in SFFD-PBS mixture (1 : 1 v/v), under the microscope. Suspensions of MDCK cells were prepared, without the use of trypsin, as previously described (Le Grimellec et al. 1988), and labeled with 0.5–2 μM laurdan as reported by Parasassi et al. (1992). Multilamellar liposomes were prepared by mixing the appropriate amount of lipids (dimyristoylphosphatidylcholine with or without cholesterol) dissolved in chloroform/methanol (1 : 1 v/v) with laurdan (laurdan/-lipid ratio = 0.5%), then evaporating the solvent under nitrogen flow. The dried samples were resuspended by vortexing in water at 37 °C in the presence of glass beads.

### Co-localization experiments

*Labeling of endosomes.* BSA-rhodamine and laurdan were added simultaneously to the medium at a final concentration of 13 μg/ml and 2 μM, respectively. Cells were incubated for 60 min, in the dark, at 37 °C, washed, and examined at 37 °C under the microscope.

Labeling of mitochondria and of the Golgi apparatus: A field of cells labeled with laurdan was selected and the images corresponding to laurdan fluorescence at 440 nm and 490 nm were recorded. The same field was imaged following 30 sec–2 min labeling with 1.1 μg/ml $DIOC_{6\,(3)}$, a marker of both mitochondria and endoplasmic reticulum (Terasaki 1989; Bergeron et al. 1994). The size of mitochondria unambiguously distinguished them from the endoplasmic reticulum. For the labeling of the Golgi apparatus, we either used the same protocol, replacing $DIOC_{6\,(3)}$ by $C_6$-NBD-Ceramide (5 μg/ml) or the probe was added simultaneously with laurdan (BODIPY TR ceramide).

### Fluorescence ratio imaging microscopy

Fluorescence ratio imaging microscopy (Bright et al. 1989; Dunn et al. 1994) was performed using an inverted epifluorescence microscope (IMT-2 with IMT2-RFL, Tokyo, Japan) equipped with a DApo 100× UV PL (1.3 N. A.) objective. Excitation light was supplied from 200 W mercury-xenon lamp (Oriel Corp., C. T.). Two filterwheels, the first equipped with neutral density filters, the second with a choice of 10 nm bandpass filters, and an electronic shutter (Vincent Assoc., Rochester, NY) were placed in the excitation light path. A manual sliding mount equipped with bandpass filters was placed in the emission path. The emission fluorescence was imaged by a Newvicon camera (sensitivity $10^{-6}$ Lux, LHESA, France) coupled with an Argus-10 (Hamamatsu, Japan) for image accumulation and acquisition and a BIOCOM 500 station (BIOCOM, France) for image analysis. Using a neutral density filter which cuts out 50% of the excitation intensity, the signal emitted by cells labeled with laurdan and illuminated continuously was stable over the first 15 sec at 440 and 490 nm. The time required for the acquisition of the pair of 440 and 490 nm images was 7 sec. For laurdan, the excitation wavelength was 360 nm (10 nm bandpass filter, Oriel Corp.). The 400 nm dichroic mirror with 420 nm barrier filter was from Olympus. The two 20 nm bandpass filters 440 DF20 and 490 DF20 for laurdan emission were purchased from Omega Optical, Brattleboro, VT). For co-localization experiments, the rhodamine filter cube combination from Olympus was used for endocytic vesicles. For $DIOC_{6\ (3)}$, the excitation light was filtered by a 485 nm, 10 nm bandpass, filter (dichroic mirror 510 nm), whereas NBD-labeled specimens were excited by irradiation at 450 nm (50 nm bandpass) and the fluorescence was observed at 520–560 nm. Photomicrographs of laurdan distribution in cells were obtained using Tri-X film (Kodak), without the neutral density filter and with a broadband emission filter (peak 480 nm, 60 nm bandpass). Images from the workstation were obtained using a videoprinter (SONY UP-811, Japan). The calculated (Lansing Taylor and Salmon 1989) depth of the field of the 1.3 NA objective (oil immersion n = 1.5) was 0.24 μm. However, this narrow depth of field did not exclude out of focus fluorescence of emitters present in the volume illuminated by the illumination cone. To determine the apparent depth of the fluorescent field 1.11 and 3.46 μm fluorescent beads (fluoresbrite carboxylate microspheres, Polysciences Inc., Warrington, PA) were used. From the ratio ($I/I_0$) of the fluorescence intensity of the larger bead at the level of best focus for the smaller bead (I) to the fluorescence intensity at its own best focus ($I_0$), the estimated apparent depth of the fluorescent field, using $I/I_0 = [\sin (u/4)/(u/4)]^2$ where $u/4 = (\pi z NA^2)/2\lambda$ (Young 1989), was ~0.8 μm, i. e., fluorescent emitters localized up to 0.8 μm above and below the focal plane contributed to the fluorescence intensity collected.

### Image processing

The generalized polarization GP was calculated using $GP = (I_{440} - I_{490})/(I_{440} + I_{490})$, (excitation GP) where $I_{440}$ and $I_{490}$ are the fluorescence intensities measured at the emission maxima of laurdan that are characterized by the gel and the liquid-crystalline phases, respectively (Parasassi et al. 1990, 1991).

Before each experiment, the coverslips supporting unlabeled cells were examined under the microscope to determine the intensity of autofluorescence. This autofluorescence essentially arises from nicotinamide adenine dinucleotide (NADH), riboflavin and flavin coenzymes, and varies according to the cell line and the growth conditions (Aubin 1979; Williams et al. 1994). With the concentration of laurdan used (2 μM), the influence of autofluorescence on the GP values is generally very limited (Yu et al. 1996). However, because both the autofluorescence level and the efficiency of labeling by laurdan varied from one experiment to another, in each experiment the gain of the intensifier of the camera was adjusted to supress the autofluorescence image before laurdan addition. This allowed us to ensure that autofluorescence did not significantly contribute to the fluorescence intensities determined after the probe addition. Dark counts of the imaging system at 440 nm and 490 nm were determined and substracted from the corresponding intensities obtained following labeling with laurdan.

### Spectrofluorimetry

The GP of cell suspensions and liposomes labeled with laurdan was calculated from emission spectra obtained on a SLM 4800 S spectrofluorimeter (SLM, Urbana, ILL).

## Results

### Determination of laurdan generalized polarization by FRIM

The GP of multilamellar liposomes of DMPC labeled with laurdan was determined in parallel by using a spectrofluorimeter and by fluorescence ratio imaging microscopy (FRIM). As shown by Fig. 1, determinations of GP, on the same liposome preparation, gave similar values by FRIM and by classical spectrofluorimetry. In accordance with previous work (Parasassi et al. 1994), the excitation GP value in the gel state was high, about 0.6, and dropped towards negative values for temperatures above the gel to liquid crystal phase transition (Tc~24 °C). FRIM measurements also confirmed (Parasassi et al. 1994) that cholesterol (33 mol/%) slightly increased the GP values at low temperature and blunted the gel to liquid crystal transition, leading to a liquid ordered state of high GP value for the range of temperature studied (Fig. 1, inset). Comparison of the GP values determined by spectrofluorimetry and by

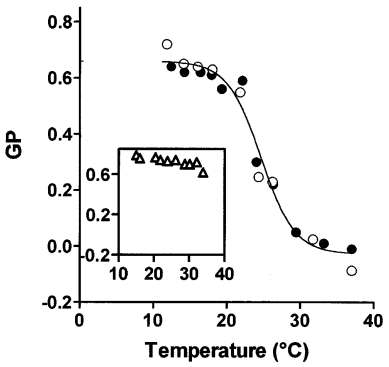


**Fig. 1** Determination of laurdan GP in multilamellar liposomes of DMPC by fluorescence ratio imaging microscopy. The generalized polarisation of multilamellar liposomes of dimyristoyl-phosphatidylcholine labeled with laurdan (laurdan/DMPC ratio = 0.5%, mol/mol) was determined as a function of temperature, on the same preparation, either by FRIM (○) or by spectrofluorimetry (●). *Inset:* GP of Cholesterol/DMPC liposomes (33 mol% cholesterol) labeled with laurdan as determined by FRIM

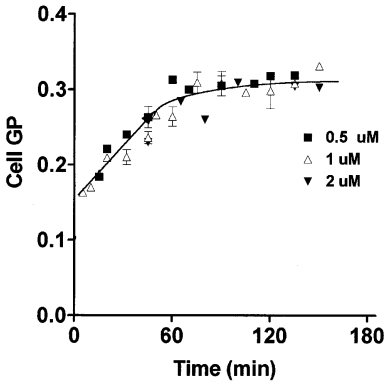


**Fig. 2** Time-dependence of GP in MDCK cell suspensions. Cells were suspended ($2\times10^5$ cells/ml) in phosphate-buffered saline containing 2 mM L-glutamine, pH 7.4. Labeling was achieved by adding, at 37 °C, under gentle stirring, laurdan (0.5 – 2 μM, final concentration) into the fluorimeter cuvette. Cell GP was determined at 37 °C, after blank subtraction

FRIM was then performed using suspensions of living MDCK cells. The cells were incubated for various times with the probe, in the fluorimeter cuvette, in PBS supplemented with glutamine (Le Grimellec et al. 1988). As shown by Fig. 2, in accordance with the data of Parasassi et al. (1992), the GP values significantly increased during the first 60 min of incubation, then plateaued. These GP values were found to be independent of the concentration of laurdan added, in the 0.5 – 2 μM range, which argues against probe-probe interactions even at the highest concentration used. The mean value determined at equilibrium by spectrofluorimetry was GP = 0.32±0.02. This value was similar to that obtained, on the same preparation of cells, by FRIM, 0.29±0.04 (n = 19 cells) which confirmed the validity of the microscopic technique for GP determinations. The images of laurdan fluorescence, however, revealed that laurdan not only labeled the plasma membrane but also intracellular membranes: when using a well established plasma membrane marker, like TMA-DPH, only the periphery of cells is labeled, giving characteristic images (Fig. 3 B, see also Le Grimellec et al. Fig. 3, 1988). In contrast, labeling with laurdan was diffuse and heterogeneous (Fig. 3 A), which indicated that a large part of laurdan was localized intracellularly. Accordingly, the GP values determined from intact cells contain contributions from both the plasma membrane and the various intracellular membranes.

## Distribution of laurdan in attached living cells

MDCK cells grown as a confluent monolayer on glass coverslips and labeled with 0.5 – 2 μM laurdan by incubation in the growth medium during 60 min at 37 °C were then examined. These 4 – 5 days cultures show zones of large and flat cells which were selected for imaging. As shown by Fig. 4, an intense labeling of intracellular structures by laurdan was observed which again strongly dif-

**Fig. 3 A, B** Localization of laurdan in MDCK cell suspensions. **A** Cells labeled for 60 min at 37 °C with 0.5 μM laurdan. For comparison, MDCK cells labeled with 0.5 μM TMA-DPH are presented in **B**. *Bar*, 25 μm

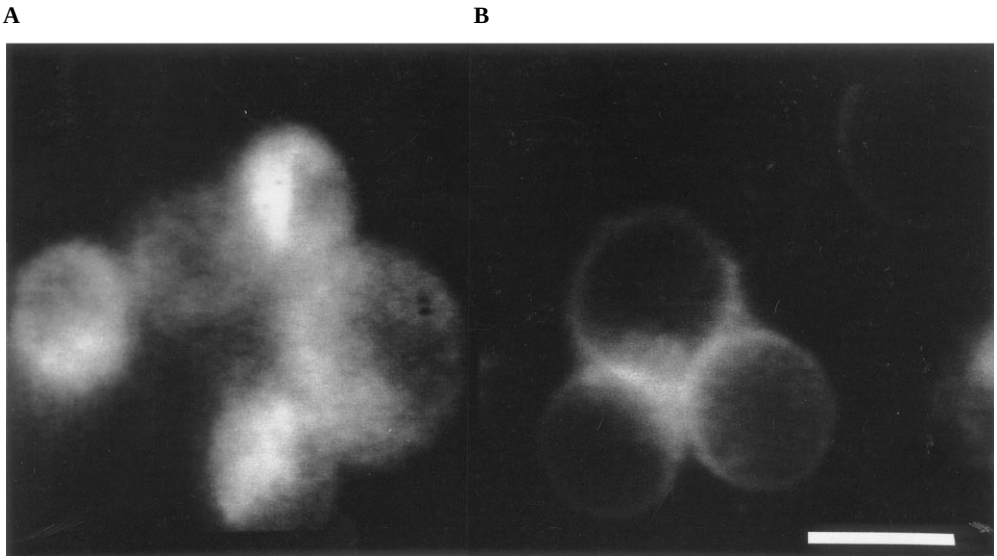

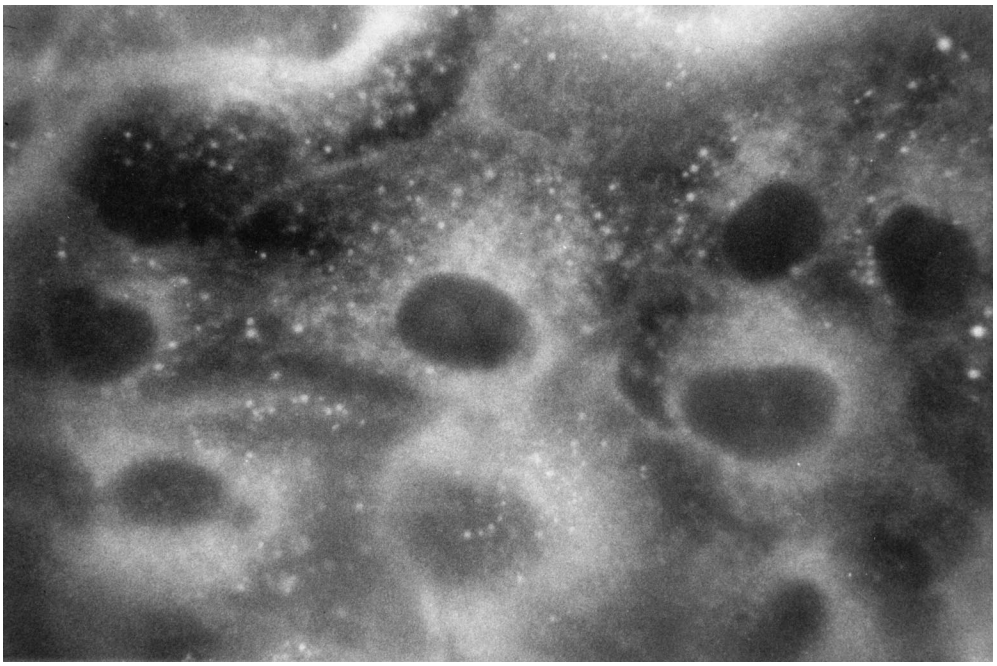

**Fig. 4** Localization of laurdan in MDCK cell monolayers. Coverslips of confluent monolayers of cells were incubated with 2 μM laurdan, at 37 °C, for 60 min. Micrograph was taken with 400 ASA Kodak Tri-X Pan film. *Bar,* 25 μm

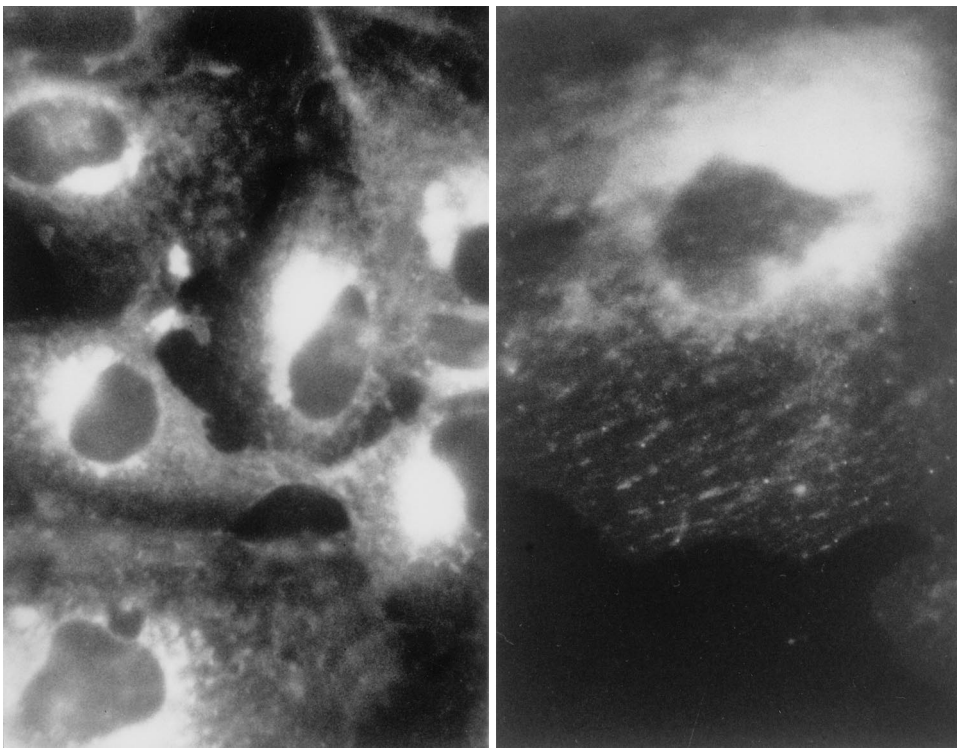

**Fig. 5** Localization of laurdan in CV-1 cells. Coverslips of non-confluent monolayers of cells were labeled with 2 μM laurdan for 60 min, at 37 °C. Micrographs were taken with 400 ASA Kodak Tri-X Pan film. Note that in this cell line laurdan seems to concentrate strongly in a perinuclear zone (Golgi apparatus?). Both plasma membrane and intracellular structures are labeled. *Left:* low magnification image. *Bar*, 50 μm. *Right:* details of one cell showing aligned structures

fered from the images obtained with TMA-DPH on the same cells (see Fig. 8, Le Grimellec et al. 1988). Except for the presence of very bright dots corresponding to an accumulation of the probe in structures which, from their appearance in phase-contrast microscopy likely corresponded to intracellular lipid droplets, and that were frequently observed in cell cultures, the fluorescence intensity of intracellular membranes was rather homogeneous. By comparison, the plasma membrane appeared only slightly labeled. Examination under the microscope of the time course of the labeling revealed that, as soon as it became detectable, i. e., about 5 min after the fluorophore addition, the fluorescence distribution in MDCK cell monolayers was comparable to that observed after 60 min incubations. This strongly suggested that the labeling of intracellular membranes was not due to the internalization of

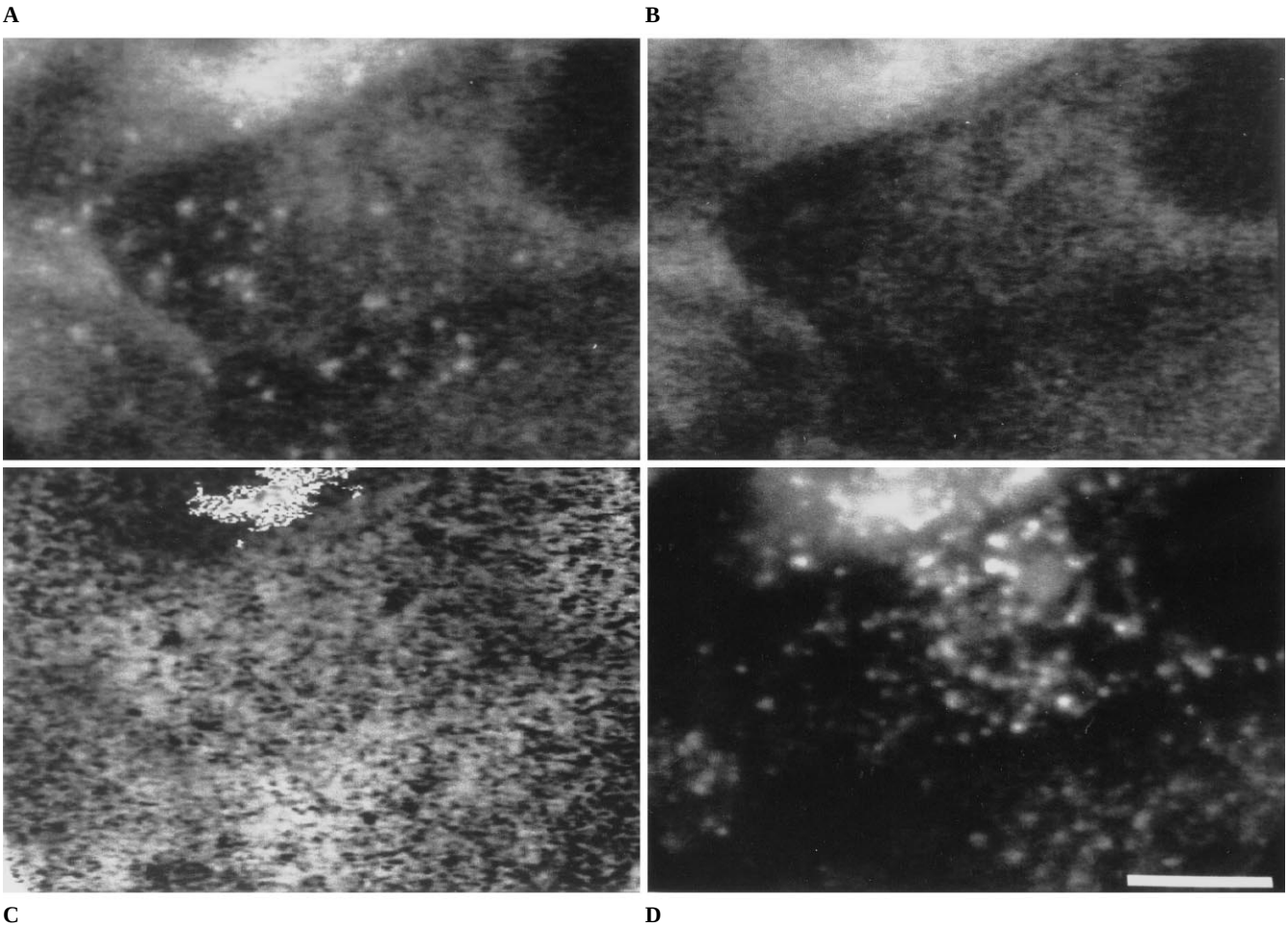


**Fig. 6 A–D** Fluorescence ratio imaging of laurdan in MDCK cells and labeling with BSA-Rhodamine. **A** Fluorescence imaging at 440 nm; **B** Fluorescence imaging at 490 nm; **C** Corresponding GP; **D** Image of endosomes labeled with BSA-Rhodamine. *Bar*, 10 μm

laurdan via endocytic processes. Moreover, preincubation of cells for 30 min at 37 °C in a medium made hyperosmotic (550 mOsm/L) by sucrose addition, a situation which practically totally inhibits endocytosis (Giocondi et al. 1995), had no effect on the distribution of laurdan in MDCK cells. Two other renal epithelial cell lines, the OK cells and the LLC-PK1 cells, gave similar images (not shown). Because they grow as still larger and flatter cells, both plasma membrane and intracellular membrane labeling was even better demonstrated using CV-1 cells, a fibroblast-like cell line originating from the kidney (Fig. 5).

## Values of cellular laurdan GP

$GP_{cell}$ mean values, at 37 °C, for 4 day cultures of living MDCK cells, MDCK cell clone 34, LLC-PK1 cells, and CV-1 cells attached to glass coverslips were, at equilibrium, 0.38±0.01, 0.22±0.01, 0.33±0.03 and 0.06±0.01, respectively. This confirmed the large heterogeneity of the membrane physical state, and likely, lipid composition, between different cell types, which was previously reported by using DPH, a probe which also labels intracellular membranes (Grunberger et al. 1982). Even for a single cell type, the individual GP values determined from the cells contained within a single microscope field of one monolayer often varied significantly (±20%). This might correspond to cells in different phase cycles (Shinitzky 1984). This also might correspond to cells in a different metabolic state: inhibition of cell metabolism by 10 mM deoxyglucose and exposure to $N_2$ resulted in a significant increase in $GP_{cell}$ (from 0.28±0.01 to 0.41±0.01, $P<0.05$, $MDCK_{cl.34}$ cells). Besides this intercellular heterogeneity, GP determinations by FRIM allowed us to estimate, in living cells, the physical state of membranes at the subcellular level. Figure 6 represents the digitized images of a monolayer of MDCK cells labeled by laurdan with the emission at 440 nm (A) and at 490 nm (B), and the corresponding GP (C). The GP map indicated that, within in a single cell, the intracellular GP values varied from 0.0 to 0.6, i. e., from the equivalent of a liquid-crystalline state to a gel or a lipid-ordered state, and that there was a marked heterogeneity in the spatial distribution of the GP values. The bright-dots likely corresponding to “lipid droplets”, when present, had very high GP values, generally between 0.5 and 0.6, indicative of their local low water content. In

spite of their characteristic high GP values, these structures which clearly appear in the images acquired at 440 nm could not be identified from the GP maps only (Fig. 6 C).

GP values of specific organelles

Accordingly, co-localization experiments with recognized markers of intracellular organelles were performed in order to identify their corresponding membrane physical state in situ, at 37 °C. These experiments were performed on attached MDCK cells, grown to confluence. For mitochondria, the 440 and 490 nm emission images of cells labeled with laurdan were recorded just before the addition of $DIOC_{(6)}$. The same field was then imaged with the appropriate filter combination and the GP corresponding to the localization of mitochondria determined. Figure 7 provides an example of this type of experiment. Small areas (10 – 20 pixels) in the center of the structures were used for GP determinations in order to limit the effects of possible mitochondrial movements between the image acquisitions. BODIPY TR ceramide (60 min incubation in the presence of laurdan) and BSA-Rhodamine (60 min incubation in the presence of laurdan) were used to identify the Golgi apparatus (Fig. 8) and the endosomes (Fig. 6), respectively. Some experiments were also performed using NBD-ceramide, using a protocol identical to that followed for $DIOC_{(6)}$. For BODIPY-ceramide and BSA-rhodamine, the position of corresponding organelles was checked before and after the acquisition of laurdan images. Only those structures that had not moved significantly were analysed. To standardize the data, results have been expressed as the ratio of the $GP_{org}$ determined for the selected organelle to the total $GP_{cell}$ of the corresponding cells. For the cell monolayers assayed, the mitochondrial mean GP value was equal to the cellular GP ($GP_{mito.}/GP_{cell} = 0.99 \pm 0.01$, $n = 238$). In contrast, the GP values of the Golgi apparatus were significantly lower than the corresponding cellular GP ($GP_{Gol.}/GP_{cell} = 0.83 \pm 0.02$, $n = 89$). The values obtained from NBD-ceramide experiments were similar to those obtained when using BODIPY TR ceramide. The GP ratio of endosomes to total cell body was significantly higher than unity (GP end./GP cell = $1.16 \pm 0.02$, $n = 95$). In these experiments, the absence of a significant correlation between the fluorescence intensities of laurdan and BSA-Rhodamine further reinforced the view that endocytosis was not responsible for the labeling of intracellular structures by the lipidic probe. As shown by Fig. 9, endosomes localized near the plasma membrane were found to have a higher GP ($GP = 0.44 \pm 0.02$, $n = 34$) than those localized near the cell nucleus ($GP = 0.24 \pm 0.02$; $n = 34$). In this series of experiments the $GP_{cell}$ was $0.31 \pm 0.04$. Finally, the generalized polarization of the plasma membrane (PM) was significantly higher than the $GP_{cell}$, $GP_{PM}/GP_{cell} = 1.52 \pm 0.05$, ($n = 11$, $MDCK_{cl.34}$ cells).

**Fig. 7 A – C** Determination of GP in mitochondria. **A** Labeling of mitochondria with $DIOC_{(6)}$. **B** and **C** Corresponding images of laurdan at 440 nm and 490 nm, respectively. *Bar,* 25 μm

## Discussion

The present experiments strongly suggest that fluorescence ratio imaging microscopy using laurdan as a probe provides access to the in situ determination of the physical state of intracellular membranes of living cells. Maps of the laurdan generalized polarization at the scale of a single cell, coupled with co-localization experiments, demonstrate the marked heterogeneity of the intracellular membrane physical state in living cells. The experiments further suggest that, at 37 °C, the GP values decreased in the following order, plasma membrane > endosomes > mitochondria > Golgi apparatus. The possibility of estimating the physical state of membranes in situ, under physiological conditions, by FRIM using laurdan as a probe pro-

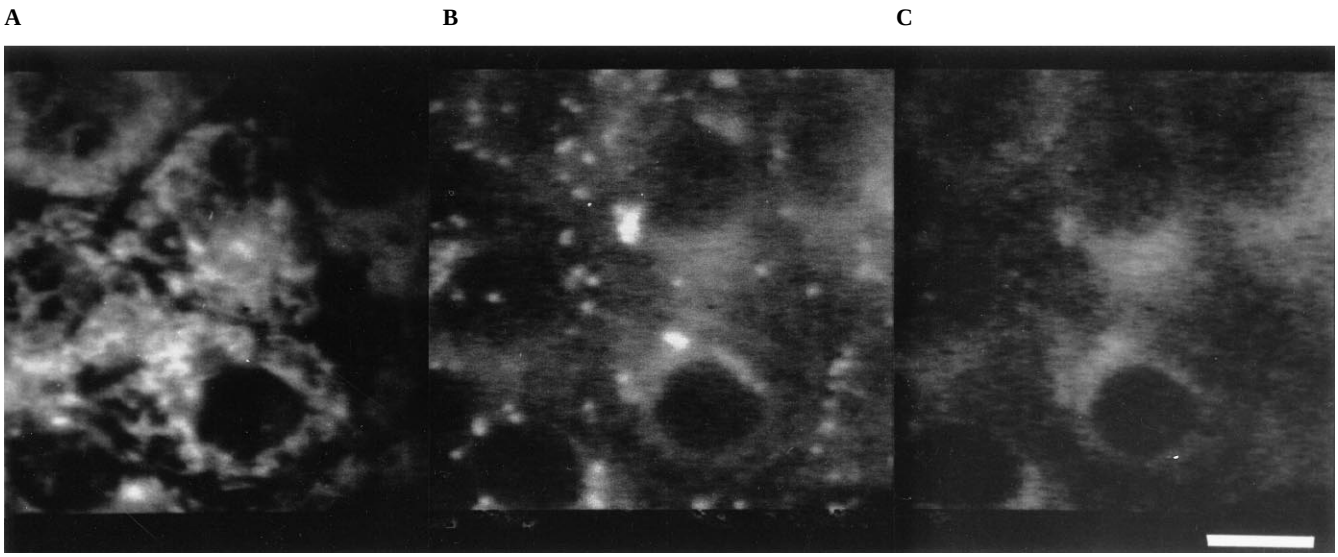

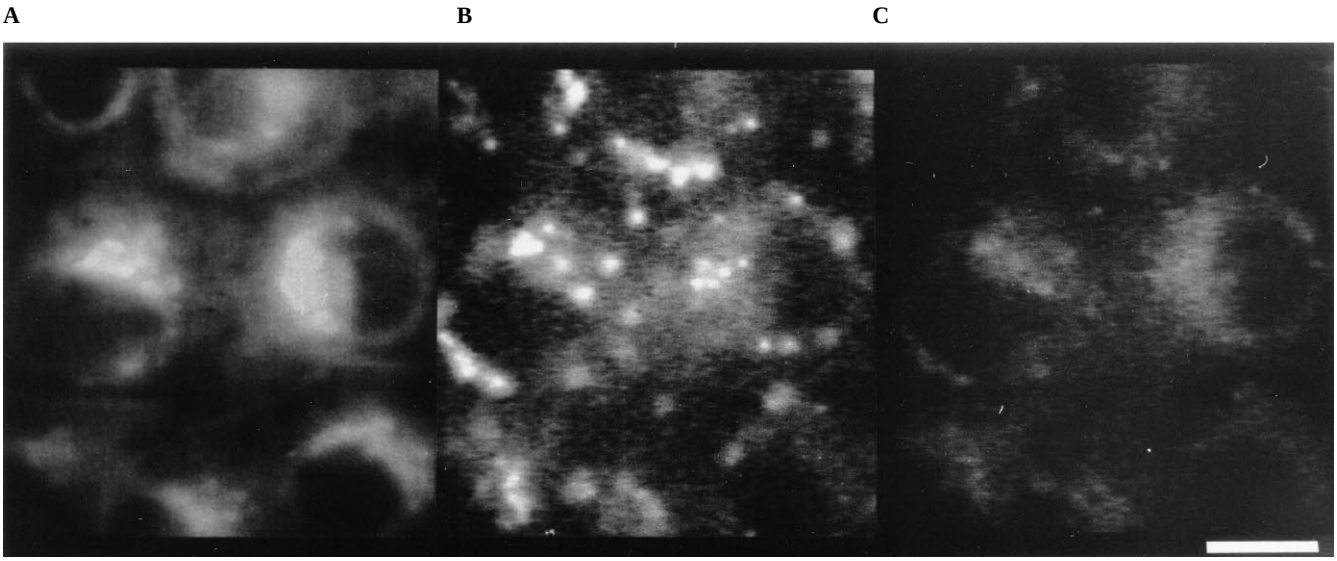


**Fig. 8 A–C** Determination of GP in the Golgi apparatus. **A** Labeling of Golgi apparatus with NBD-Cer. **B** and **C** Corresponding images of laurdan at 440 nm and 490 nm, respectively. *Bar*, 25 μm

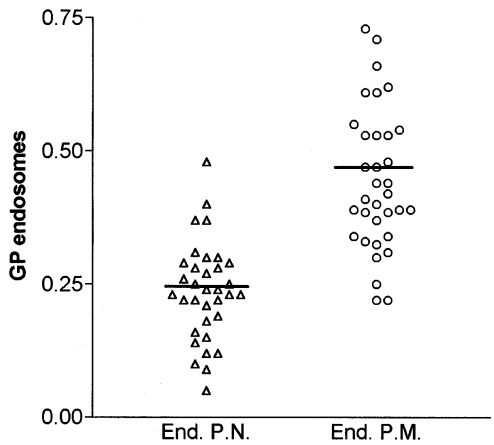


**Fig. 9** Difference in GP between perinuclear and peripheral endosomes. The GP of BSA-Rhodamine labeled structures close to the nucleus (End. P. N.) or close to the plasma membrane (End. P. M.) was determined from three different experiments on different cell batches

vides a promising tool for elucidating the relationships between membrane physico-chemical properties and cell biology.

Previous studies from Parasassi et al. have established on model systems that the generalized polarization of laurdan is a potent probe of membrane physical state (Parasassi et al. 1990, 1991, 1992). Owing to the marked sensitivity of laurdan to the polarity and to the molecular dynamics of dipoles in its environment, a 50 nm red shift of the emission maximum is obtained when lipids pass from the gel to liquid-crystalline phase. In fact, the emission shift reflects the local modification in the water content that is associated with the change in membrane physical state (Parasassi and Gratton 1995). This potentially makes laurdan a very suitable tool for ratio imaging fluorescence microscopy, a powerful technique that has been applied to the study of the regulation of intracellular ions at the level of a single cell as well as at the subcellular level (for reviews, see Bright et al. 1989; Dunn et al. 1994). In the present experiments, the GP values obtained by spectrofluorimetry and by FRIM, as a function of the temperature, for dimyristoylphosphatidylcholine liposomes labeled with laurdan were similar, indicating that GP can be accurately determined by FRIM. This was confirmed using living MDCK cells in suspension where the mean cell GP value determined by FRIM was also similar, despite a significant dispersion of individual cell values, to that obtained, from the same suspension, by spectrofluorimetry. In accordance with spectrofluorimetry data on various cell suspensions (Parasassi et al. 1992, 1993; Liu et al. 1995), the mean GP values, obtained at 37 °C by FRIM, of attached cells were found to vary significantly as a function of the cell type, for instance from values close to zero for CV-1 cells to values around 0.4 for MDCK cells. Large differences in the membrane physical state of living cells according to the cell type, the age of the cells, the stage of the cell cycle were reported by investigators who used DPH as a probe (for a review see Shinitzky 1984). For a given cell type, the scattering of GP values of individual cells under the same microscope field might be explained by such differences in their stage of the cycle. In addition, differences in the metabolic state of the cells might also contribute to the GP intercellular heterogeneity as suggested by the change in GP induced by metabolic inhibition.

It is now well established that the DPH anisotropy values thus obtained corresponded not only to the plasma membrane but also to intracellular membranes (Grunberger et al. 1982). The same situation was found for laurdan that not only labeled the plasma membrane but also intracellular membranes of the various kidney cells. This intracellular labelling was made particularly clear by compar-

ing the images obtained with laurdan to those obtained when using TMA-DPH, a recognized marker of the plasma membrane of MDCK cells and of numerous other cell lines. Intracellular labeling of comparable distribution but of lower intensity was detected a few minutes after the probe addition. This suggested that laurdan did not enter the cells via endocytic processes, which would have resulted in a selective labeling of intracellular organelles. This hypothesis was confirmed using the inhibition of endocytosis by a hyperosmotic sucrose medium (Giocondi et al. 1995), which did not modify the labeling pattern. Labeling of kidney cell intracellular membranes by laurdan agrees with the data of Yu et al. (1996) obtained in mouse fibroblast cells. Thus, it is likely that laurdan permeates through the plasma membrane and diffuses into the intracellular membranes as do many other uncharged lipids or lipidic probes, such as diphenylhexatriene.

Accordingly, for laurdan, the GP values determined on intact cells, rather than the GP value of the plasma membrane, correspond to $GP_{cell} = \alpha_{pm}GP_{pm} + \Sigma\alpha_i GP_i$ were $\alpha_{pm}$ and $GP_{pm}$ represent the fraction of laurdan present in the plasma membrane and its corresponding GP, and $\Sigma\ \alpha_i GP_i$ is the contribution of the various intracellular membranes.

The cellular GP maps were highly heterogeneous, with local GP values close to those obtained in a liquid-crystalline phase whereas others were typical of the gel or liquid-ordered state. However, as shown for the "lipidic droplets", the different intracellular organelles could not be identified from a characteristic GP value only. In other words, setting a laurdan GP value did not allow us to define the contour of a well defined organelle because the GP values varied within a single organelle. Although membrane microheterogeneity might be involved in these variations, a more likely explanation comes from the fact that the GP determined for an organelle localized in the focal plane contains contributions from laurdan molecules embedded in other intracellular membranes located above and below the organelle. Thus, as for the $Gp_{cell}$, the $GP_{org}$ we determined corresponded to $Gp_{org} = \alpha_{org}\ Gp_{org} + \Sigma\alpha_i GP_i$ were $\alpha_{org}$ and $GP_{org}$ represent the fraction of laurdan present in the chosen organelle and its corresponding GP, and $\Sigma\alpha_i GP_i$ is the contribution of the various other intracellular membranes in the volume of fluorescence emission. Accordingly absolute quantitative assessment of $GP_{org}$ is actually out of reach of the technique and local variations in the type and the abundance of intracellular membranes located around the organelle chosen will influence the GP value determined at different positions of the organelle. Still, to be representative or to give a reasonable estimate of the specific GP of an organelle requires that $\alpha_{org}\ GP_{org} \gg \Sigma\alpha_i GP_i$. The observation that co-localization experiments with established markers of intracellular organelles gave GP mean values characteristic for each type of organelle strongly suggests this was the case. For the "lipidic droplets" for instance, the GP values measured between 0.5 and 0.6 were close to the maximum value we obtained for DMPC in the gel phase. An important contribution of intracellular membranes would have significantly lowered these values. An explanation, at least partial, for the limited influence of the other intracellular membranes on the GP of chosen organelles might be in the limited height of the cells. Except for the nucleus region, the large MDCK cells we observed, which likely correspond to the MDCK-1 cell subtype, are rather flat with a mean cellular height of 1 μm (Kersting et al. 1993) and with regions as thin as 0.3 – 0.4 μm (Ojakian et al. 1987). It is noteworthy that this height is significantly smaller than the apparent depth of the fluorescent field we determined with the fluorescent beads and is comparable to the height of the focal plane in two-photon fluorescence microscopy (Williams et al. 1994). For the plasma membrane, the apparent GP values obtained strongly suggested that the plasma membrane of living cells is significantly more ordered than intracellular membranes. This agrees with the high order of the plasma membrane detected by using TMA-DPH in living MDCK cell monolayers (Le Grimellec et al. 1988) and with the fact that most of the cellular cholesterol is located in the plasma membrane of cells (Lange 1991; El Yandouzi et al. 1994). The membrane of endosomes, identified from the internalization of fluorescently labeled BSA, had a mean GP value intermediate between the plasma membrane GP and the $Gp_{cell}$. This resulted from the fact that rhodamine-BSA labeled structures localized near the plasma membrane had GP values significantly higher than those found around the cell nucleus. Because of the incubation time with rhodamine-BSA we cannot, however, exclude the possibility that part of the perinuclear-labeled structures might correspond to lysozomes or that, because of the thickening of the cell in the region close to the nucleus, the GP of endosomes was only apparently decreased due to an increased influence of other intracellular membranes. This last possibility would make the endosomes different from the other organelles tested whose GP was independent of the distance to the nucleus. This applied to mitochondria whose GP value in situ was found to be similar to the cell GP value whatever the position in the cell. In MDCK cells, mitochondria fill a major part of the intracellular space (see Fig. 7 and Bergeron et al. 1994). The mitochondrial membranes, as most of the intracellular membranes, generally contain very low amounts of cholesterol. Thus the relatively high lipid order of mitochondria, in MDCK cells, suggested by GP values around 0.3, can hardly be accounted for by a "liquid ordered" phase induced by cholesterol. Fluorescence polarization studies with DPH suggested that the membrane fluidity of isolated mitochondria, and more generally of the various intracellular membranes, is high (Shinitzky and Inbar 1976; Pottel et al. 1983; van Blitterswijk et al. 1987). On the other hand, quenching experiments with 2,4,6-trinitrobenzene sulfonate or N-bixinoyl glucosamine of DPH-labeled cells indicate that, in situ, the average physical state of intracellular membranes is close to the membrane physical state determined on the intact cell (Grunberger et al. 1982). This suggests that mitochondrial membranes, and more generally intracellular membranes, in situ might have physical properties different from those determined on corresponding isolated structures. The mean GP

value obtained from the structure labeled with either NBD- or BODIPY-ceramide was significantly lower than the $GP_{cell}$. These two probes are vital stains of the Golgi apparatus of cells (Lipsky and Pagano 1985; Pagano et al. 1991). Again, the Golgi GP was independent of the distance between the nucleus and the GP determination site. Although the presence of cholesterol in the Golgi was detected by filipin (Orci et al. 1981), conflicting results concerning the amount of cholesterol present in Golgi membranes have been obtained from subcellular fractionation experiments (cholesterol/phospholipid ratio from <0.1 up to 0.5 mol/mol; Taylor et al. 1984; Brasitus et al. 1988; Kadowaki et al. 1994). Our data therefore strongly suggest that, in situ, the amount of cholesterol interacting with membrane phospholipids in the Golgi apparatus of MDCK cells is low. This is in accordance with the observation by Urbani and Simoni (1990) that the delivery to the plasma membrane of cholesterol bypasses the Golgi apparatus.

Taken together these data strongly suggest that laurdan is a promising tool for studies on the relationships between membrane physical state and intracellular trafficking. They also indicate that common fluorescence ratio imaging microscopy equipment can be used for such determinations when using relatively flat cultured cells.

**Acknowledgements** Part of this work was supported by "La Fondation pour la Recherche Médicale", "La Région Languedoc-Roussillon", and the ARC association. We want to thank Christine Leroy for providing us with the cloned MDCK cells (MDCK Cl.34).

## References

Aubin JE (1979) Autofluorescence of viable cultured mammalian cells. J Histochem Cytochem 27: 36–43

Bergeron M, Thiéry G, Lenoir F, Giocondi M-C, Le Grimellec C (1994) Organization of the endoplasmic reticulum in renal cell lines MDCK and LLC-PK1. Cell Tissue Res 277: 297–307

Brasitus TA, Dahiya R, Dudeja PK (1988) Rat proximal small intestinal Golgi membranes: lipid composition and fluidity. Biochim Biophys Acta 958: 218–226

Bright GR, Fisher GW, Rogowska J, Taylor DL (1989) Fluorescence ratio imaging microscopy. Methods in Cell Biol 30: 157–192

Dunn KW, Mayor S, Myers JN, Maxfield FR (1994) Applications of ratio fluorescence microscopy in the study of cell physiology. FASEB J 8: 573–582

El Yandouzi EH, Zlatkine P, Moll G, Le Grimellec C (1994) Cholesterol distribution in renal epithelial cells LLC-PK1 as determined by cholesterol oxydase: Evidence that glutaraldehyde fixation masks plasma membrane cholesterol pools. Biochemistry 33: 2329–2334

Fiorini R, Curatola G, Bertoli E, Giorgi PL, Kantar A (1990) Changes of fluorescence anisotropy in plasma membrane of human polymorphonuclear leukocytes during the respiratory burst phenomenon. FEBS Lett 273: 122–126

Giocondi M-C, Friedlander G, Le Grimellec C (1990) ADH modulates plasma membrane lipid order of living MDCK cells via a cAMP-dependent process. Am J Physiol 259: F95–F103

Giocondi M-C, Mamdouh Z, Le Grimellec C (1995) Benzyl alcohol differently affects fluid phase endocytosis and exocytosis in renal epithelial cells. Biochim Biophys Acta 1234: 197–202

Gordon LM, Mobley PW (1985) Membrane lipids, membrane fluidity and enzyme activity. In: Aloia RC, Boggs JM (eds) Membrane fluidity in biology, vol 4. Academic Press, Orlando, pp 1–49

Grunberger D, Haimovitz R, Shinitzky M (1982) Resolution of plasma membrane fluidity in intact cells labelled with diphenylhexatriene. Biochim Biophys Acta 688: 764–774

Illinger D, Poindron D, Glasser N, Modollel M, Khury J-G (1990) The plasma membrane internalization and recycling upon activation with gamma-interferon and lipopolysaccharide; a study using the fluorescent probe trimethylaminodiphenylhexatriene. Biochim Biophys Acta 1030: 82–87

Illinger D, Khury J-G (1994) The kinetic aspects of intracellular fluorescence labeling with TMA-DPH support the maturation model for endocytosis in L929 cells. J Cell Biol 125: 783–794

Kadowaki H, Grant MA, Seyfried TN (1994) Effect of Golgi membrane phospholipid composition on the molecular species of GM3 gangliosides synthesized by rat liver sialyltransferase. J Lipid Res 35: 1956–1964

Kersting U, Schwab A, Treidtel M, Pfaller W, Gastraunthaler G, Steigner W, Oberleithner H (1993) Differentiation of Madin-Darby Canine Kidney cells depends on cell culture conditions. Cell Physiol Biochem 3: 42–55

Khury J-G, Duportail G, Bronner C, Laustriat G (1985) Plasma membrane fluidity measurements on whole living cells by fluorescence anisotropy of trimethylammoniumdiphenylhexatriene. Biochim Biophys Acta 845: 60–67

Lange Y (1991) Disposition of intracellular cholesterol in human fibroblasts. J Lipid Res 32: 329–339

Lansing Taylor D, Salmon ED (1989) Basic fluorescence microscopy. Methods in Cell Biology 29: 207–237

Le Grimellec C, Friedlander G, Giocondi M-C (1988) Asymmetry of plasma membrane lipid order in Madin-Darby Canine Kidney cells. Am J Physiol 255: F22–F32

Le Grimellec C, Friedlander G, El Yandouzi EH, Zlatkine P, Giocondi M-C (1992) Membrane fluidity and transport properties in epithelia. Kidney Int 42: 825–836

Levi M, Wilson PV, Cooper OJ, Gratton E (1993) Lipid phases in renal brush border membranes revealed by laurdan fluorescence. Photochem Photobiol 57: 420–425

Lipsky NG, Pagano RE (1985) Intracellular translocation of fluorescent sphingolipids in cultured fibroblasts: Endogenously synthesized sphingomyelin and glucocerebroside analogues pass through the Golgi apparatus en route to the plasma membrane. J Cell Biol 100: 27–34

Liu Y, Cheng DK, Sonek GJ, Berns MW, Chapman CF, Tromberg BJ (1995) Evidence for localized cell heating induced by infrared optical tweezers. Biophys J 68: 2137–2144

Mouritsen OG, Bloom M (1993) Models of lipid-protein interactions in membranes. Annu Rev Biophys Biomol Struct 22: 145–171

Ojakian GK, Romain RE, Herz RE (1987) A distal nephron glycoprotein that has different cell surface distributions on MDCK cell sublines. Am J Physiol 253: C433–C443

Orci L, Montesano R, Meda P, Malaisse-Lagae F, Brown D, Perrelet A, Vassali P (1981) Heterogeneous distribution of filipin-cholesterol complexes across the cisternae of the Golgi apparatus. Proc Natl Acad Sci USA 78: 293–297

Pagano RE, Martin OC, Kang HC, Haugland RP (1991) A novel fluorescent ceramide analogue for studying membrane traffic in animal cells: accumulation at the Golgi apparatus results in altered spectral properties of the sphingolipid precursor. J Cell Biol 113: 1267–1279

Parasassi T, De Stasio G, d'Ubaldo A, Gratton E (1990) Phase fluctuation in phospholipid membranes revealed by laurdan fluorescence. Biophys J 57: 1179–1186

Parasassi T, De Stasio G, Ravagnan G, Rusch RM, Gratton E (1991) Quantitation of lipid phases in phospholipid vesicles by the generalized polarization of laurdan fluorescence. Biophys J 60: 179–189

Parasassi T, Di Stefano M, Ravagnan G, Sapora O, Gratton E (1992) Membrane aging during cell growth ascertained by laurdan generalized polarization. Exp Cell Res 202: 432–439

Parasassi T, Loiero M, Raimondi M, Ravagnan G, Gratton E (1993) Absence of lipid gel-phase domains in seven mammalian cell lines and in four primary cell types. Biochim Biophys Acta 1153: 143–154

Parasassi T, Di Stefano M, Loiero M, Ravagnan G, Gratton E (1994) Influence of cholesterol on phospholipid bilayers phase domains as detected by laurdan fluorescence. Biophys J 66: 120–132

Pottel H, van der Meer W, Herreman W (1983) Correlation between the order parameter and the steady-state fluorescence anisotropy of 1,6-diphenyl-1,3,5-hexatriene and an evaluation of membrane fluidity. Biochim Biophys Acta 730: 181–186

Prendergast FG, Haugland RP, Callahan PJ (1981) 1-[4-(Trimethylamino)phenyl]-6-phenylhexatriene: Synthesis, fluorescence properties, and use as a fluorescence probe of lipid bilayers. Biochemistry 20: 7333–7338

Sheridan NP, Block ER (1988) Plasma membrane fluidity measurements in intact endothelial cells: effect of hyperoxia on fluorescence anisotropies of 1-[4-(trimethylamino)phenyl]-6-phenylhexa-1,3,5-triene. J Cell Physiol 134: 117–123

Shinitzky M (1984) Membrane fluidity and cellular functions. In: Shinitzky M (ed) Physiology of membrane fluidity, vol 1. CRC Press, Boca Raton, pp 1–51

Shinitzky M, Inbar M (1976) Microviscosity parameters and protein mobility in biological membranes. Biochim Biophys Acta 433: 133–149

Simons K, van Meer G (1988) Lipid sorting in epithelial cells. Biochemistry 27: 6197–6202

Storch J, Shulman SL, Kleinfeld AM (1989) Plasma membrane lipid order and composition during adipocyte differentiation of 3T3F442A cells. J Biol Chem 264: 10 527–10 533

Taylor JA, Limbrick AR, Allan D, Judah JD (1984) Isolation of highly purified Golgi membranes from rat liver use of cycloheximide in vivo to remove Golgi contents. Biochim Biophys Acta 769: 171–178

Terasaki M (1989) Fluorescent labeling of endoplasmic reticulum. Methods in Cell Biol 29: 125–135

Urbani L, Simoni RD (1990) Cholesterol and vesicular stomatitis virus G protein take separate routes from the endoplasmic reticulum to the plasma membrane. J Biol Chem 265: 1919–1923

van Blitterswijk WJ, Wieb van der Meer B, Hilkmann H (1987) Quantitative contributions of cholesterol and the individual classes of phospholipids and their degree of fatty acyl (un)saturation to membrane fluidity measured by fluorescence polarization. Biochemistry 26: 1746–1756

Williams RM, Piston DW, Webb WW (1994) Two-photon molecular excitation provides intrinsic 3-dimensional resolution for laser-based microscopy and microphotochemistry. FASEB J 8: 804–813

Yeagle PL (1993) Lipid-Protein interactions and the roles of lipids in biological membranes. In: Yeagle PE (ed) The membranes of cells. Academic Press, San Siego, pp 203–229

Young IT (1989) Image fidelity: characterizing the imaging transfer function. Methods Cell Biol 30: 1–45

Yu W, So PTC, French T, Gratton E (1996) Fluorescence Generalized polarisation of cell membranes: a two-photon scanning microscopy approach. Biophys J 70: 626–636